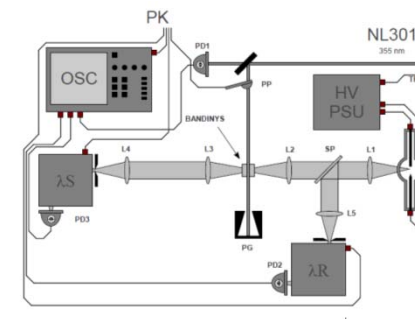


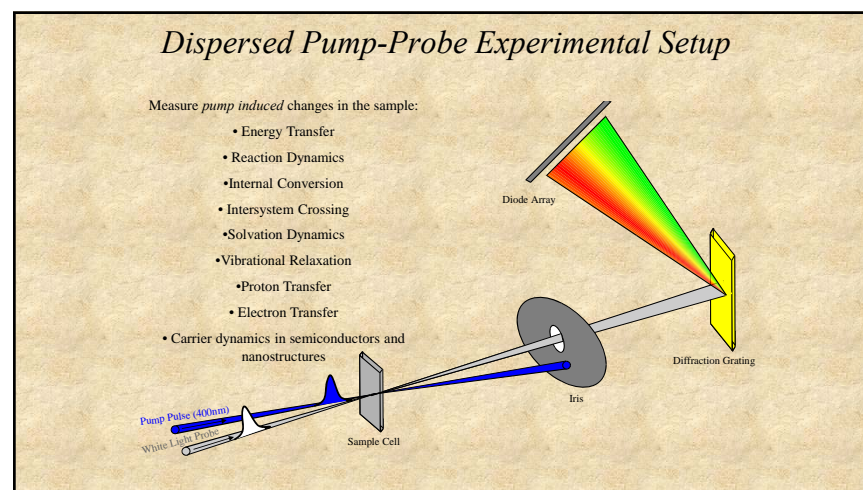
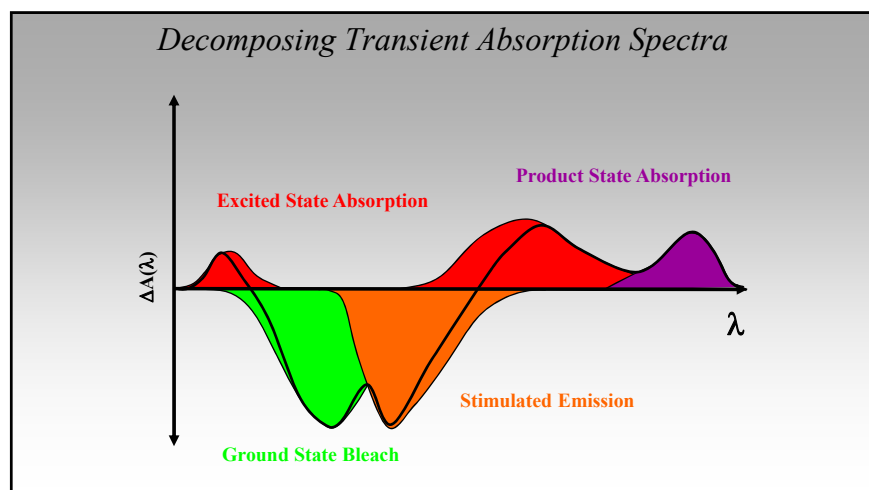
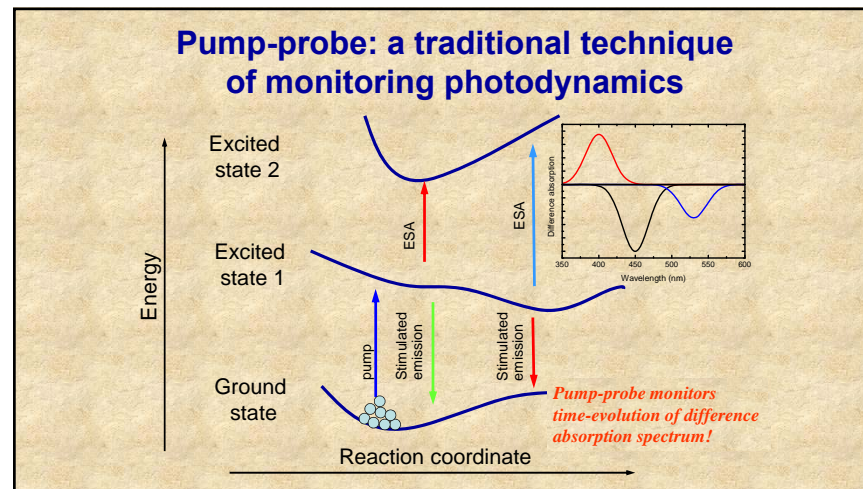
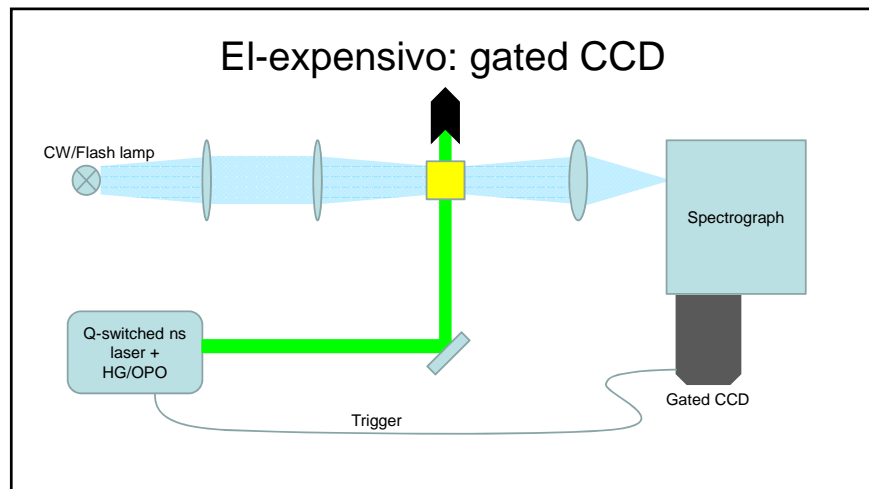
Nanoseconds – to microseconds

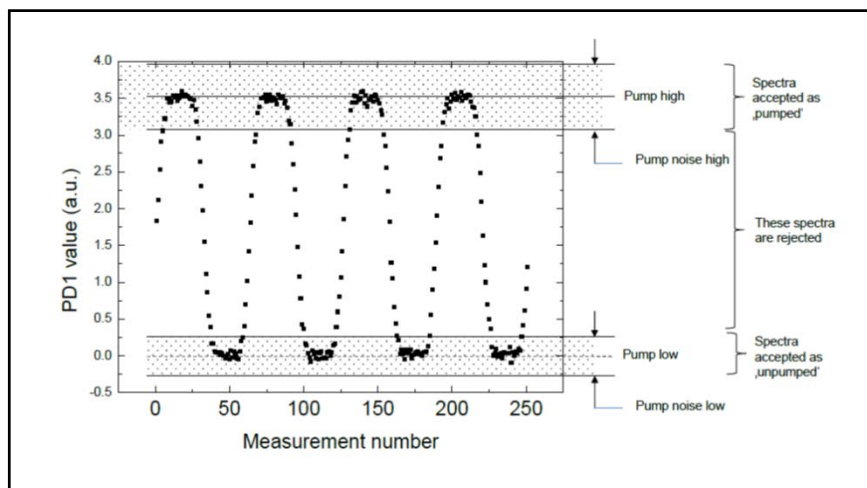
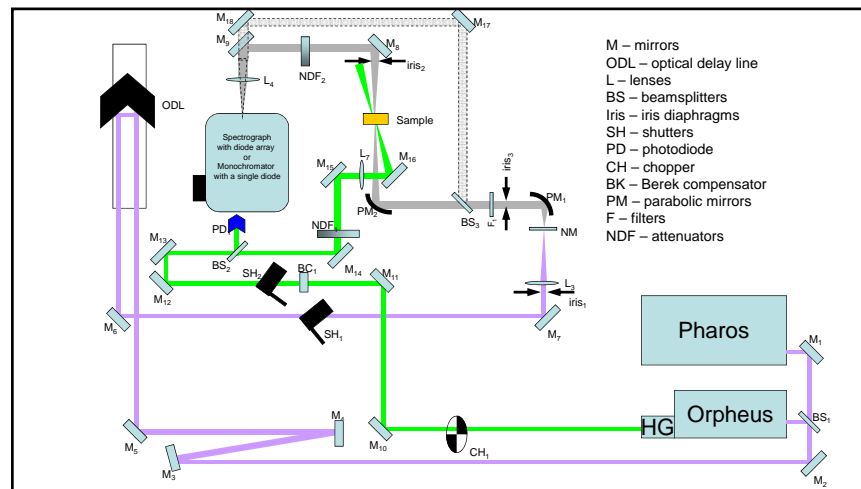
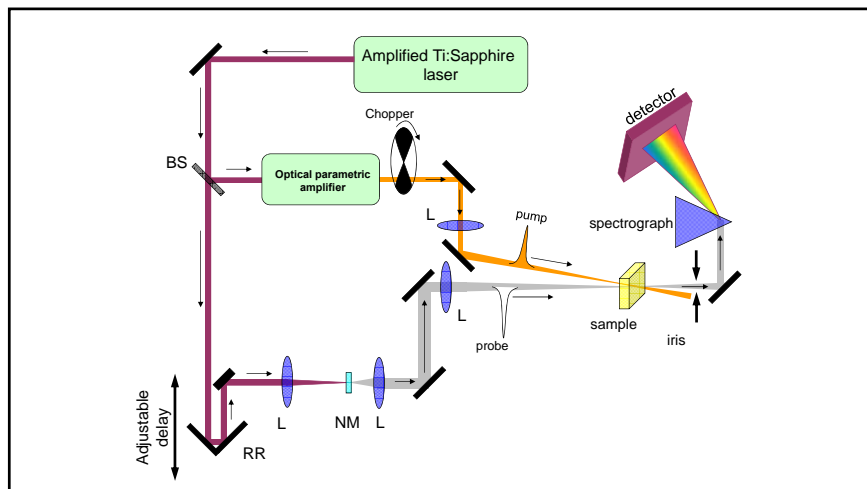
- Electronic methods with fast detectors are applied;
 - Gated CCD (expensive);
 - Oscilloscope+fast diode;
 - Synchronized femtosecond+nanosecond laser

EI-cheapo: oscilloscope+flashlamp



5 pav. Žibinto fotolės eksperimentinė schema. Kaupinimui naudojamas lazerinis šaltinis NL301, zondavimui – lazerinio kaupinimo paskirties Xe blyškė B. Bandinio sugerties polyciai registruojami pakankamą praleidžiamą dažnių juostą turinčiu oscillografiu OSC kaip fotodiodų PD2 ir PD3 signalų santykis. Fotodiodas PD1 naudojamas sinchronizacijai. Spektrinė slyva realizuojama monochromatoriais λS ir λR. lanko slyva – oscillografiu OSC. PG – pluošto gaudyklė.



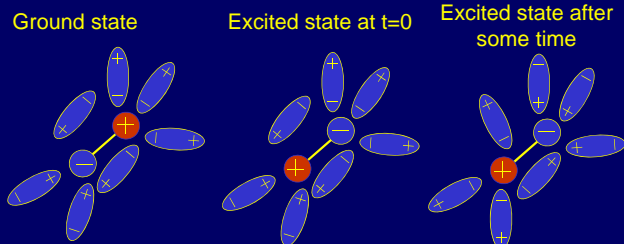


Experiment sequence

1. Measurements are done shot-to-shot
2. A buffer of shots is acquired
3. The probe intensity spectra are separated to 'pumped' and 'dark'
4. Outlier spectra are removed from pumped and dark bins
5. The pumped and dark spectra are averaged
6. Difference absorption is calculated
7. 1-6 is repeated and DOD is averaged
8. The delay line moves to a new position and the procedure in 7 is repeated;
9. 8 is repeated for a number of scans.

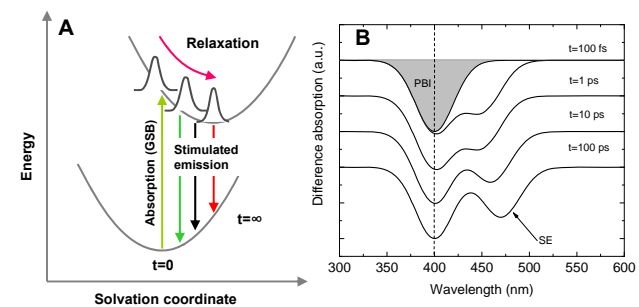
- Shots can be accumulated on-chip, if needed.

Conceptual example: solvation



Adjustment of solvent molecules around the solute to minimize the overall system energy.

Conceptual example: solvation



Laurdan: a marker molecule for probing local structure of lipid bilayers

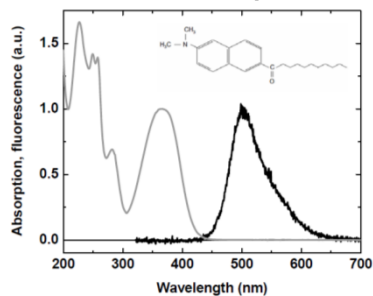


Figure 3.13 Absorption (gray line) and emission (black line) spectra together with the structural formula of membrane marker Laurdan in the methanol solution.

Laurdan: a marker molecule for probing local structure of lipid bilayers

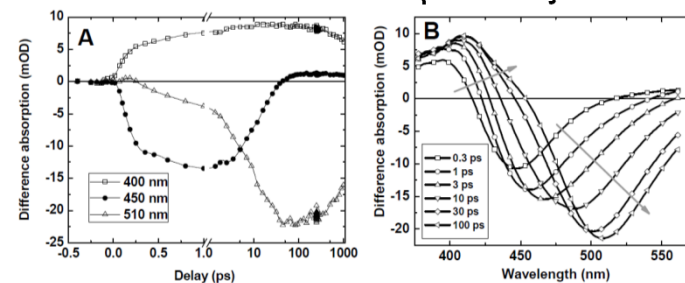
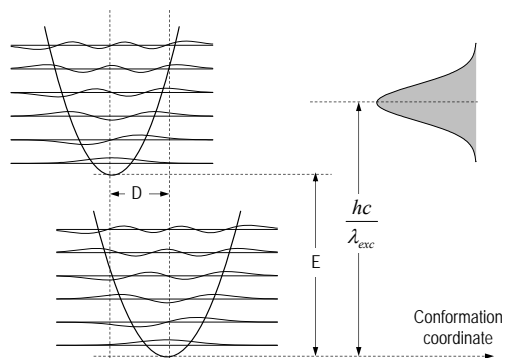


Figure 3.14 A: pump-probe traces measured on laurdan dissolved in methanol. Note that the time axis is linear up to 1 ps and logarithmic thereafter. B: difference absorption spectra measured at various delays after the excitation. Delay times are shown in the legend. Gray arrows indicate the observed trends.

Conceptual example 2: two electronic levels coupled to 1 vibrational mode



Some basic quantum mechanics...

- The pulse excites several vibrational sub-states at once (forms so-called excited-state wavepacket):

$$\Psi_{exc}(x, t) = \sum_j a_j(t) \psi_j(x)$$

Where $\psi_j(x)$ - oscillator eigenfunctions

$a_j(t)$ - time-dependent amplitudes

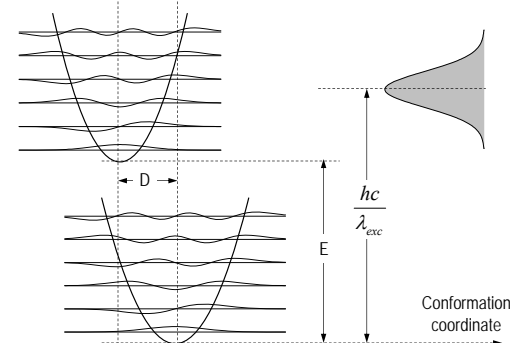
Some basic quantum mechanics...

- After plugging this into time dependent Schrödinger equation

$$i\hbar \frac{\partial}{\partial t} \Psi = \hat{H} \Psi$$

$$\cdot \psi_k^*(x), \int \dots dx \left| \begin{aligned} i\hbar \sum_j \psi_j(x) \frac{\partial}{\partial t} a_j(t) &= \hat{H} \sum_j a_j(t) \psi_j(x) \\ \frac{\partial}{\partial t} a_k(t) &= i\omega_v \left(\frac{1}{2} + k \right) a_k(t) \\ a_k(t) &= a_k(0) e^{-i\omega_v \left(k + \frac{1}{2} \right) t} \end{aligned} \right.$$

Oversimplified model system: two electronic levels coupled to 1 vibrational mode



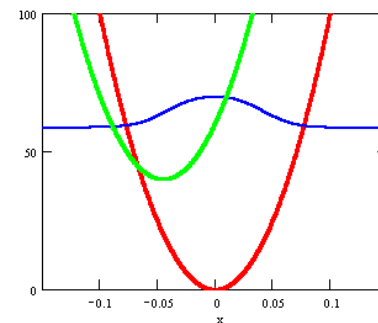
Initial population of the vibrational substates in the excited electronic state

$a_k(0)$ depend on:

- Population of ground state vibronic sublevels (Boltzmann factor);
- Overlaps between ground- and excited-state vibrational wavefunctions (Frank-Condon factors);
- Width and central frequency of the excitation pulse;

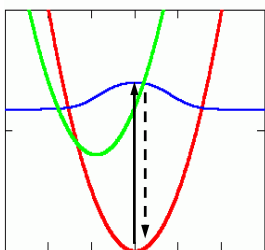
• All of this can be calculated for our model!

Example: red-edge excitation, 100 fs pulse,
77K

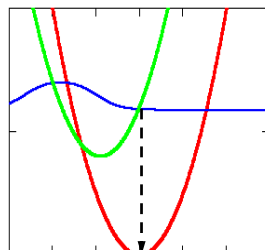


The reason for oscillations in pump-probe

Probed at time zero:



Probed after half period:



Generalization

When electron-vibronic system is excited with an ultrashort pulse (its spectrum has to cover several vibrational levels), oscillations will be observed in pump-probe time dependence, corresponding to the wavepacket motion.

Even a system with time-independent Hamiltonian will show dynamics if prepared in a coherent superposition of states.

The lifetime of these vibrations is typically hundreds of femtoseconds, even several picoseconds (corresponds to the width of vibrational lines in Raman spectrum).

Let's keep it in the back of our heads for later...

**Application:
Role of carotenoids in excitation quenching**

**Leaf response to prolonged illumination –
reduction of fluorescence**

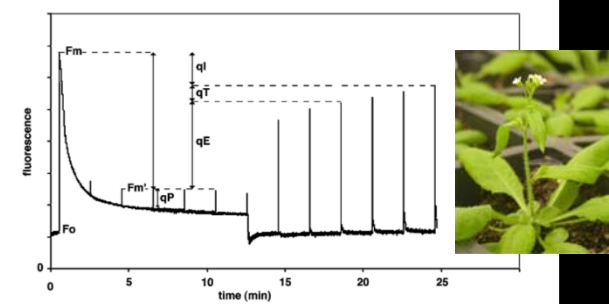
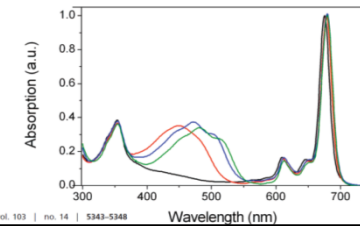
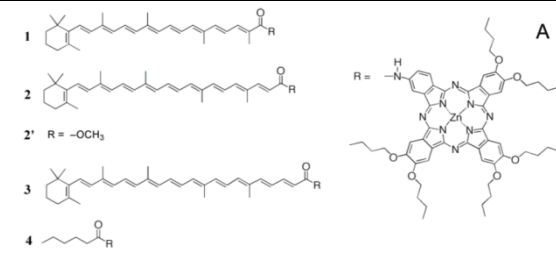
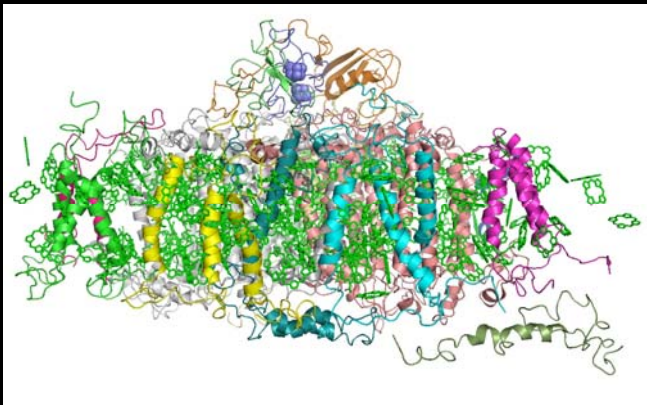


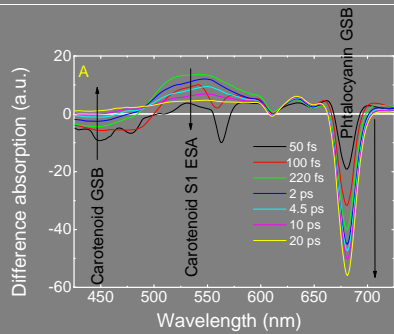
Figure 2. Chl fluorescence measurement from an Arabidopsis leaf. In the presence of only weak measuring light the minimal fluorescence (F_o) is seen. When a saturating light pulse is given, the photosynthetic light reactions are saturated and fluorescence reaches a maximum level (F_m). Upon continuous illumination with moderately excess light ($750 \mu\text{mol photons m}^{-2} \text{sec}^{-1}$; growth light was $130 \mu\text{mol photons m}^{-2} \text{sec}^{-1}$), a combination of qP and NPQ lowers the fluorescence yield. NPQ ($qE + qI + qP$) can be seen as the difference between F_m and the measured maximal fluorescence after a saturating light pulse during illumination (F_m'). After switching off the light, recovery of F_m within a few minutes reflects relaxation of the qE component of NPQ.



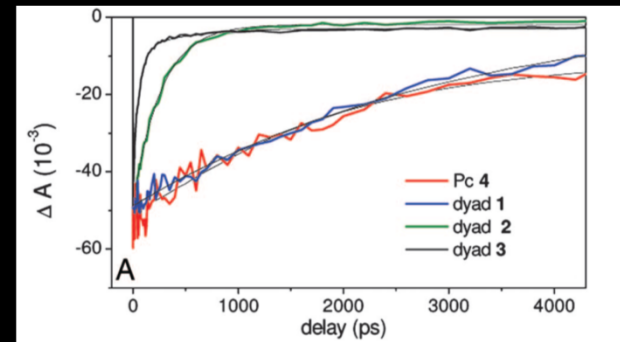
Berera et al.

PNAS | April 4, 2006 | vol. 103 | no. 14 | 5343-5348

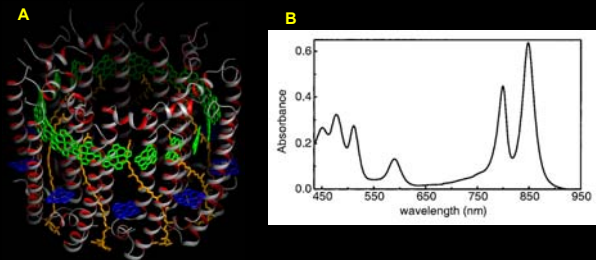
EET dynamics monitored by pump-probe spectroscopy



Carotenoid can be both energy donor and acceptor



Energy transfer in LH2 of purple bacteria



Possibilities of EET in LH2

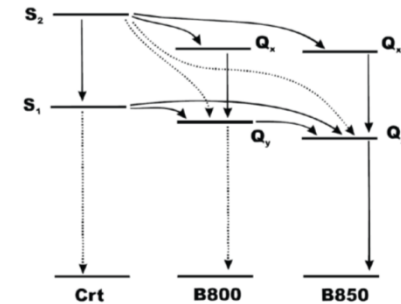


Fig. 33. Generalized scheme of energy transfer pathways in LH2. Reproduced from [28].

Energy transfer from carotenoids to bacteriochlorophylls in LH2

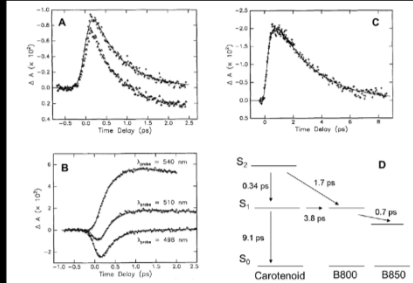
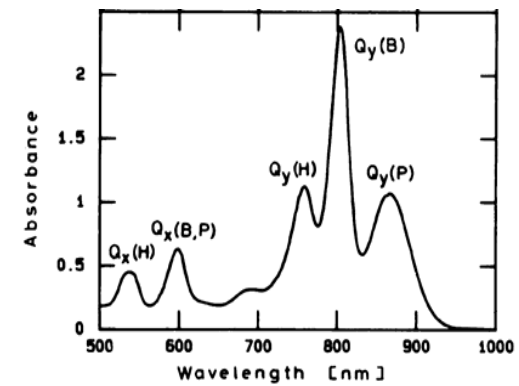
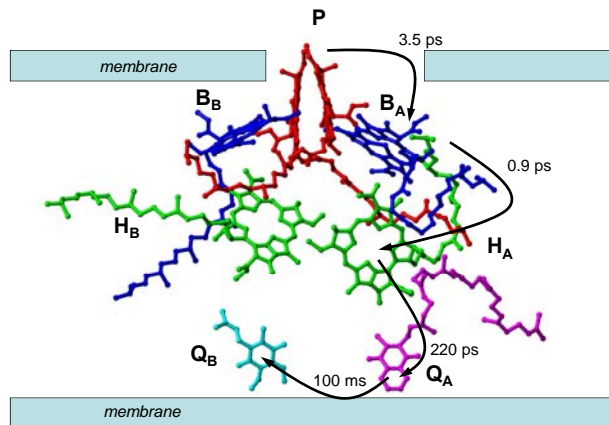
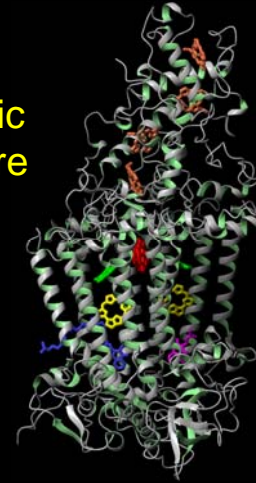
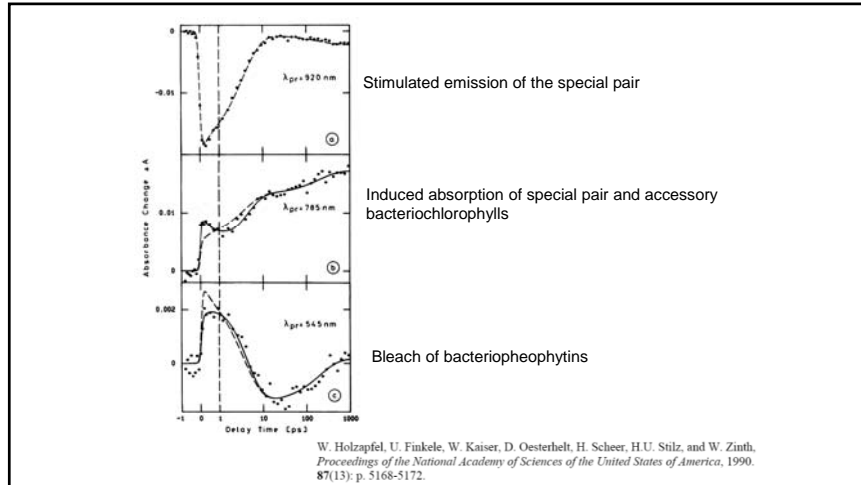


Fig. 34. Pump-probe experiment in the light-harvesting complex LH2 of *Rhodospirillum rubrum*. A: pump and probe wavelength 800 nm (triangle show experimental data, whereas 'plus' symbols correspond to the data with subtracted B850 excited state absorption, i.e. they show 'pure' GSB of B800); B: excitation wavelength - 480 nm (carotenoid S_2 absorption, see Fig. 19), probe wavelengths are shown on the graph; C: excitation wavelength - 510 nm, probe wavelength 800 nm. The data in this trace are corrected by subtracting B850 ESA signal, i.e. they represent 'pure' B800 bleach. Note the inverted vertical scale in panels A and C. D: the energy transfer times determined from the data. Reproduced from [29].

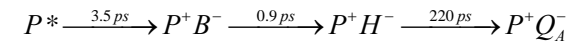
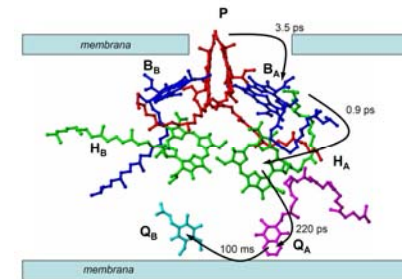
Shreve, A.P., et al., Femtosecond Energy-Transfer Processes in the B800-850 Light-Harvesting Complex of *Rhodospirillum rubrum*-2.4.1. *Biochimica Et Biophysica Acta*, 1991, 1058(2), p. 280-288.

Application: photosynthetic reaction centre

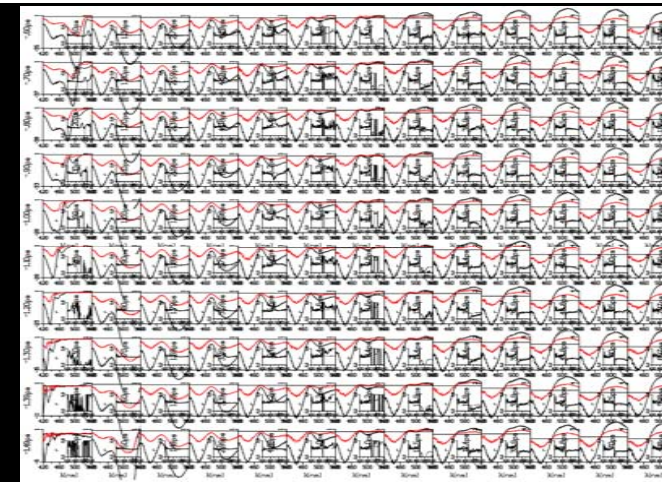




W. Zinth et al. conclusion



A word on data analysis

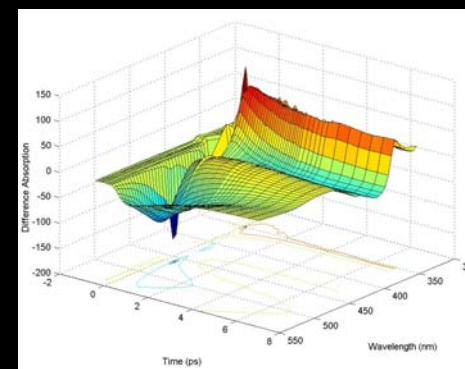


Or...

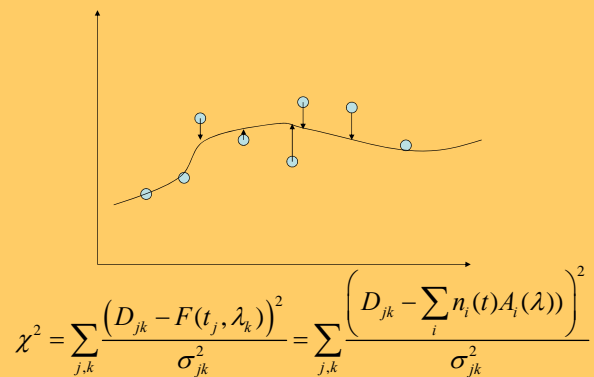


Or

Pump-probe dataset

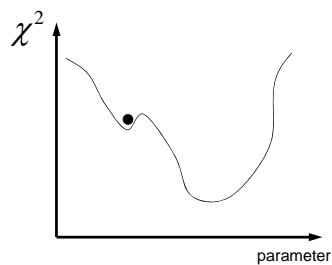


Merit function



Linear least squares

Global and local minima



Instrument response function

$$D(t) = \int_{-\infty}^{\infty} S(\tau) IRF(t - \tau) d\tau$$

Typical for time-resolved spectroscopy

$$I(t) = \frac{1}{\sqrt{2\pi z}} e^{-\frac{t^2}{2z^2}}$$

Instrument response function

$$\frac{dn}{dt} = \frac{A}{\sqrt{2\pi z}} e^{-\frac{t^2}{2z^2}} - \frac{1}{\tau_f} n$$

$$n(t) = G(t) \cdot e^{-\frac{t}{\tau_f}}$$

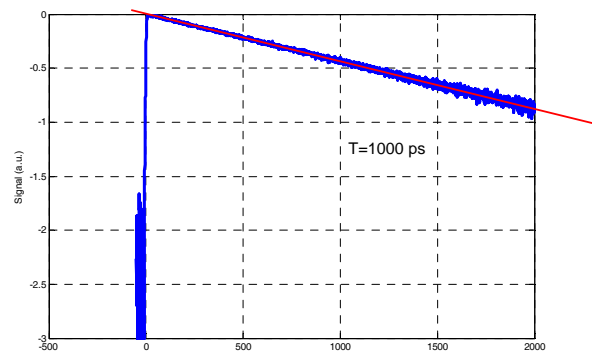
$$G(t) \sim 1 + \operatorname{erf}\left(\frac{t}{z}\right)$$

$$\operatorname{erf}(t) \equiv \frac{2}{\sqrt{\pi}} \int_0^t e^{-t^2} dt$$

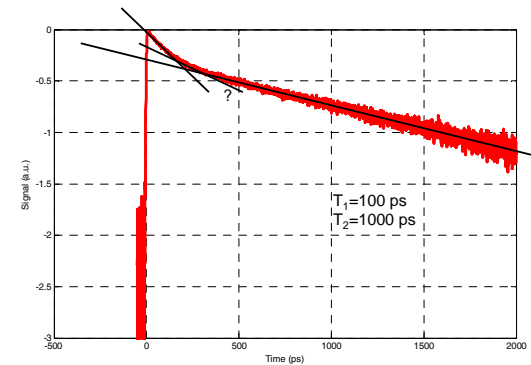
Gaussian instrument response

$$F(t, \lambda) = \frac{1}{2} \left(1 + \operatorname{erf}\left(\frac{t}{z}\right) \right) \sum_{n=1}^N A_n(\lambda) e^{-\frac{t}{\tau_n}}$$

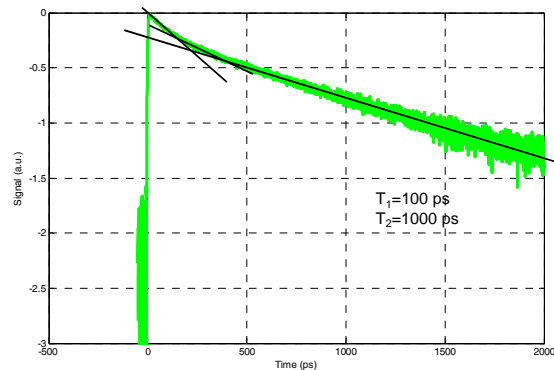
One, two three exponents



One, two three exponents



One, two three exponents



Singular value decomposition

$$\begin{pmatrix} \mathbf{A} \end{pmatrix} = \begin{pmatrix} \mathbf{U} \end{pmatrix} \cdot \begin{pmatrix} w_0 & w_1 & \dots & w_{N-1} \end{pmatrix} \cdot \begin{pmatrix} \mathbf{V}^T \end{pmatrix}$$

$$\begin{pmatrix} \mathbf{A} \end{pmatrix} = \begin{pmatrix} \mathbf{U} \end{pmatrix} \cdot \begin{pmatrix} w_0 & w_1 & \dots & w_{N-1} \end{pmatrix} \cdot \begin{pmatrix} \mathbf{V}^T \end{pmatrix}$$

$\mathbf{V} \cdot \mathbf{V}^T = \mathbf{1}$
 $\mathbf{V}^T \cdot \mathbf{V} = \mathbf{1}$
 $\mathbf{U}^T \cdot \mathbf{U} = \mathbf{1}$

$$\sum_{j=0}^{N-1} V_{jk} V_{jn} = \delta_{kn} \quad \begin{matrix} 0 \leq k \leq N-1 \\ 0 \leq n \leq N-1 \end{matrix} \quad \sum_{i=0}^{M-1} U_{ik} U_{in} = \delta_{kn} \quad \begin{matrix} 0 \leq k \leq N-1 \\ 0 \leq n \leq N-1 \end{matrix}$$

Singular value decomposition

- Divides a matrix into 'most important columns', 'most important rows' and 'importance coefficients' (singular values);
- Great for solving linear systems of equations

$$\mathbf{Ax} = \mathbf{b}$$

in least-squares sense, i.e. finds \mathbf{x} , such that

$$|\mathbf{Ax} - \mathbf{b}|$$

is minimized.

Solving linear system

$$\mathbf{A} = \mathbf{U} \cdot \text{diag}[\boldsymbol{\omega}] \cdot \mathbf{V}^T$$

$$\mathbf{V} \cdot \text{diag}\left[\frac{\mathbf{1}}{\boldsymbol{\omega}}\right] \cdot \mathbf{U}^T \cdot \mathbf{U} \cdot \boldsymbol{\omega} \cdot \mathbf{V}^T = \mathbf{1}$$

$$\mathbf{A}^{-1} = \mathbf{V} \cdot \text{diag}\left[\frac{\mathbf{1}}{\boldsymbol{\omega}}\right] \cdot \mathbf{U}^T$$

U and V columns/rows are orthogonal

$$\sum_{i=0}^{M-1} U_{ik} U_{in} = \delta_{kn} \quad \begin{matrix} 0 \leq k \leq N-1 \\ 0 \leq n \leq N-1 \end{matrix}$$

$$\sum_{j=0}^{N-1} V_{jk} V_{jn} = \delta_{kn} \quad \begin{matrix} 0 \leq k \leq N-1 \\ 0 \leq n \leq N-1 \end{matrix}$$

General linear least squares

- Linear combination of model functions:

$$y(x) = \sum_{k=0}^{M-1} a_k X_k(x)$$

- Chi square is the merit function, as before:

$$\chi^2 = \sum_{i=0}^{N-1} \left[\frac{y_i - \sum_{k=0}^{M-1} a_k X_k(x_i)}{\sigma_i} \right]^2$$

General linear least squares

- Normal equations are obtained by taking a derivative of chi square and zeroing it:

$$0 = \sum_{i=0}^{N-1} \frac{1}{\sigma_i^2} \left[y_i - \sum_{j=0}^{M-1} a_j X_j(x_i) \right] X_k(x_i)$$

$$\sum_{j=0}^{M-1} \alpha_{kj} a_j = \beta_k$$

$$\alpha_{kj} = \sum_{i=0}^{N-1} \frac{X_j(x_i) X_k(x_i)}{\sigma_i^2}$$

$$\beta_k = \sum_{i=0}^{N-1} \frac{y_i X_k(x_i)}{\sigma_i^2}$$

General linear least squares

- The system of equations constructed in such a way is called *normal equations*. Its solution is equivalent to solving the fitting problem.

$$\sum_{j=0}^{M-1} \alpha_{kj} a_j = \beta_k$$

Nonlinear least squares a.k.a Levenberg-Marquardt

- Guess initial values and look for the closest minimum...



Nonlinear least squares a.k.a Levenberg-Marquardt

- If the parameter guess is close to the minimum, use Taylor expansion to the quadratic order.
- If guess is bad – go in the direction of steepest descent.
- L-M method is a continuous variation between these two approaches.

Models are reflections of reality in our minds

Phenomenological
Intuitive
Simplistic
Good description of data

Complicated
First principles based
Meaningful
Unintuitive
Far away from data



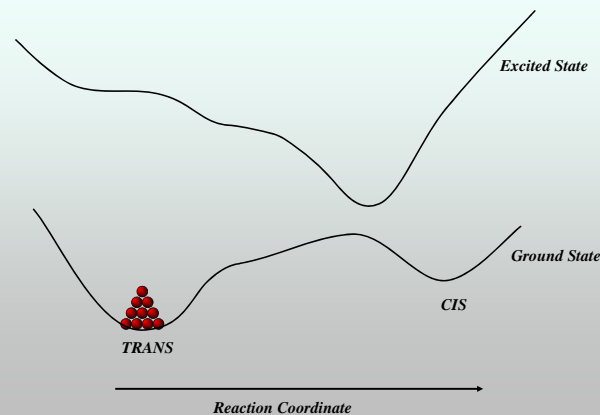
$$\begin{aligned}
 R_1(t_1, t_2, t_1) &= \sum_{abcd} P(\alpha) \mu_{ad} \mu_{bc} \exp[i\bar{\omega}_{ab} t_1 + i\bar{\omega}_{cd} t_2 - i\bar{\omega}_{bc} t_1 + F_{abcd}^{(1)}(t_1, t_2, t_1)] \\
 R_2(t_1, t_2, t_1) &= \sum_{abcd} P(\alpha) \mu_{ad} \mu_{bc} \mu_{ba} \exp[i\bar{\omega}_{ab} t_1 + i\bar{\omega}_{cd} t_2 + i\bar{\omega}_{ba} t_1 + F_{abcd}^{(2)}(t_1, t_2, t_1)] \\
 R_3(t_1, t_2, t_1) &= \sum_{abcd} P(\alpha) \mu_{ad} \mu_{bc} \mu_{ba} \mu_{cb} \exp[i\bar{\omega}_{ab} t_1 + i\bar{\omega}_{cd} t_2 + i\bar{\omega}_{ba} t_1 + i\bar{\omega}_{cb} t_2 + F_{abcd}^{(3)}(t_1, t_2, t_1)] \\
 R_4(t_1, t_2, t_1) &= \sum_{abcd} P(\alpha) \mu_{ad} \mu_{bc} \mu_{ba} \mu_{cb} \mu_{ca} \exp[i\bar{\omega}_{ab} t_1 + i\bar{\omega}_{cd} t_2 + i\bar{\omega}_{ba} t_1 + i\bar{\omega}_{cb} t_2 + i\bar{\omega}_{ca} t_1 + F_{abcd}^{(4)}(t_1, t_2, t_1)]
 \end{aligned}$$

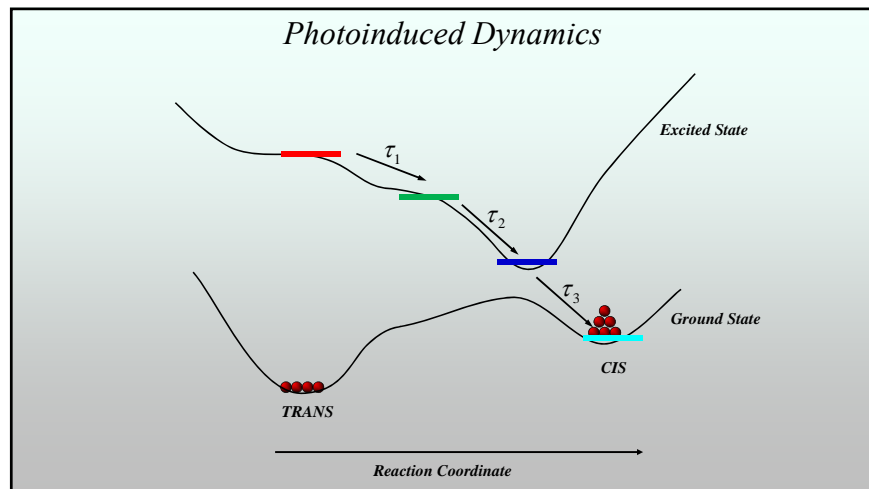
$$\begin{aligned}
 P_{3D}(\mathbf{r}, t) &= N \int_0^\infty dt_3 \int_0^\infty dt_2 \int_0^\infty dt_1 R_{3D}(t_3, t_2, t_1) \\
 &\times \mathbf{E}(\mathbf{r}, t - t_3) \mathbf{E}(\mathbf{r}, t - t_3 - t_2) \times \mathbf{E}(\mathbf{r}, t - t_3 - t_2 - t_1) \quad (4)
 \end{aligned}$$

$$\begin{aligned}
 \tilde{R}_i^{++}(\Omega_1, t_2, \Omega_2) &= \int_{-\infty}^{\infty} dt_1 \int_{-\infty}^{\infty} dt_2 R_i(t_1, t_2, t_1) e^{i(\Omega_1 t_1 + \Omega_2 t_2)} \\
 &= \sum_{abcd} P(\alpha) \mu_{ad} \mu_{bc} \mu_{ba} \mu_{cb} \int_{-\infty}^{\infty} dt_1 \int_{-\infty}^{\infty} dt_2 \exp\{i(\bar{\omega}_{ab} + \Omega_1)t_1 + i\bar{\omega}_{cd} t_2 - i(\bar{\omega}_{bc} - \Omega_2)t_1\} \\
 &\times \exp\{i(t_2) - \frac{1}{2}\delta_1^2(t_1)t_1^2 - \frac{1}{2}\delta_2^2(t_2)t_2^2\} \\
 &= \sum_{abcd} P(\alpha) \mu_{ad} \mu_{bc} \mu_{ba} \mu_{cb} \left(\begin{array}{c} \mu_{ad} \\ \mu_{bc} \\ \mu_{ba} \\ \mu_{cb} \end{array} \right) P_D(T) + \left(\begin{array}{c} \mu_{ad} \\ \mu_{bc} \\ \mu_{ba} \\ \mu_{cb} \end{array} \right) P_A(T)
 \end{aligned}$$

Hole Exciton Hole Exciton

Photoinduced Dynamics

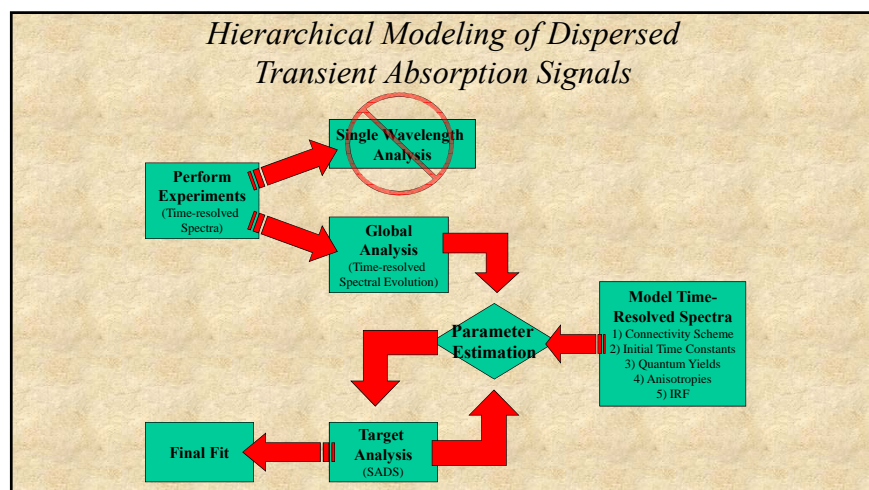




Global analysis is a 'pinball machine' approximation of ultrafast data

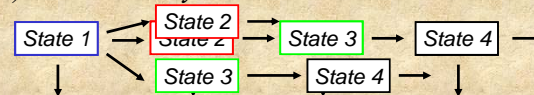
Use it when:

- You do not know any better.
- You need to parametrize large datasets concisely.
- You need to present and interpret the data to people without hardcore physics background.



Three Principle Objectives of Global Analysis

1) Connectivity



2) Timescales

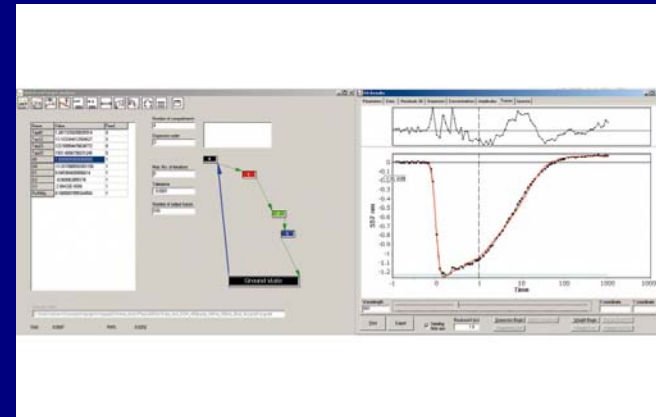
$$\dot{n}_i(t) = \sum_j k_{ij} n_j(t)$$

3) Spectra

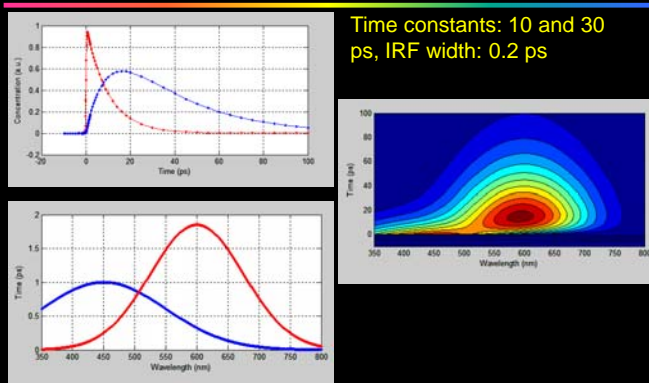
$$D(\lambda, t; k_{ij}) = \sum_i A_i(\lambda) n_i(t; k_{ij})$$

Available options:

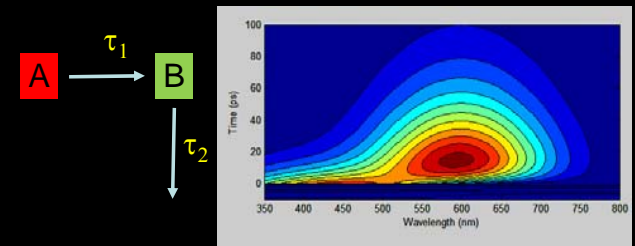
- Glotaran – VU Amsterdam
- CarpetView –  LIGHT CONVERSION
- Jasper van Thor's Matlab® based package
- A number of groups have developed their own software



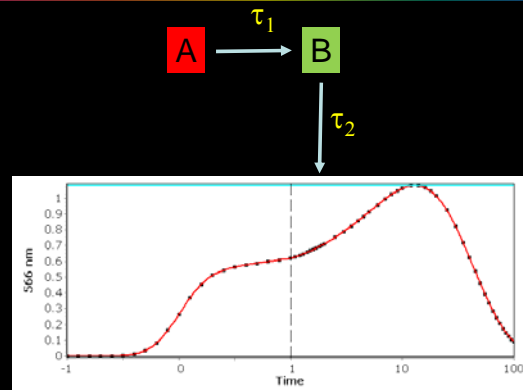
Time-resolved fluorescence dataset (fake data)



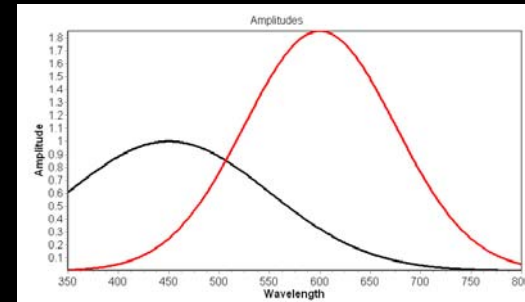
Let's fit it using sequential model...



Let's fit it using sequential model...



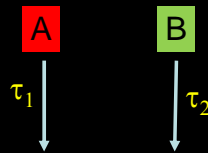
Let's fit it using sequential model...



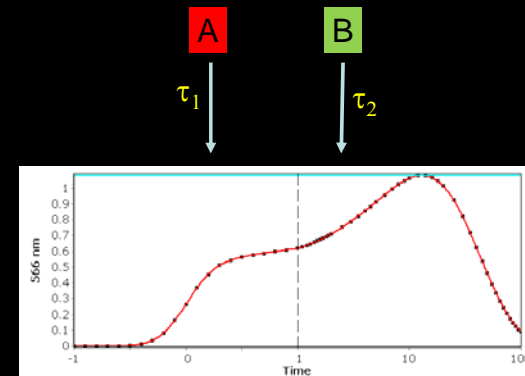
Time constants: 10 and 30 ps,
IRF width: 0.2 ps, just what we put in. **So, we nailed it, right?...**

WRONG.

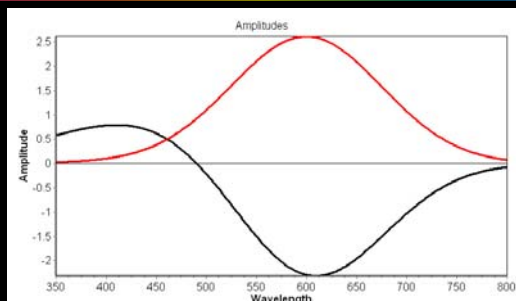
To see why, let's fit it using another model:



The fit is just as good

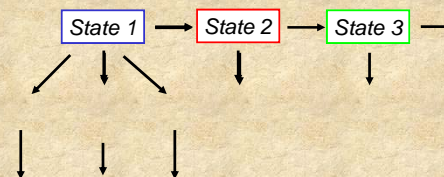


But the component spectra look different:

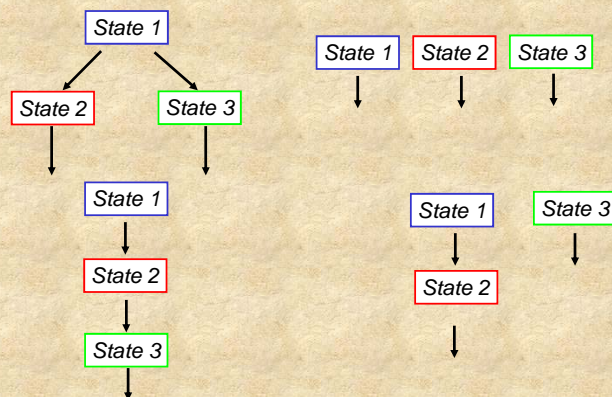


The models represent two different realities, they can't both be correct.

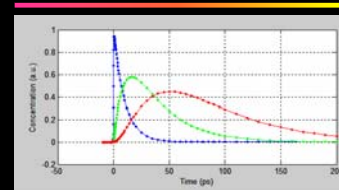
Imagine what you could do with three-component models:



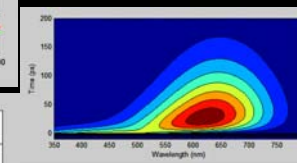
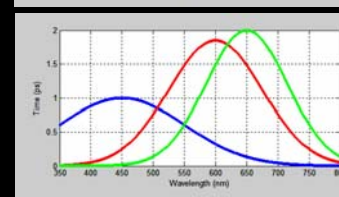
Imagine what you could do with three-component models:

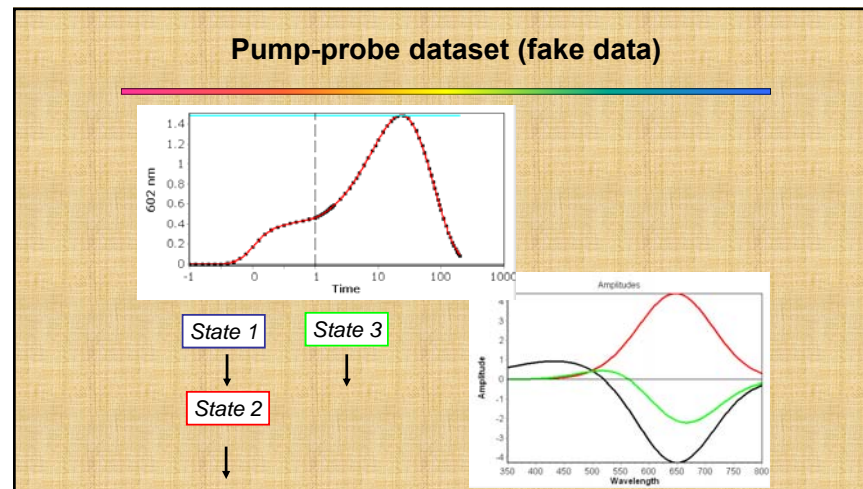
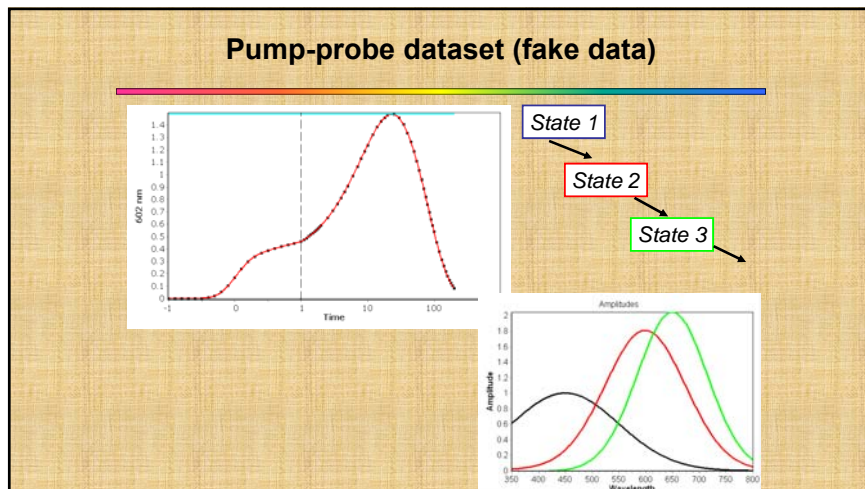


Fluorescence dataset (fake data)



Time constants: 10, 30 and 50 ps, IRF width: 0.2 ps





Model degeneracy

- Any model using connectivity scheme with the same rank (number of different lifetimes observed) will fit the data equally well.
- Besides the quality of the fit, the models have to be judged by the plausibility of component spectra they produce!

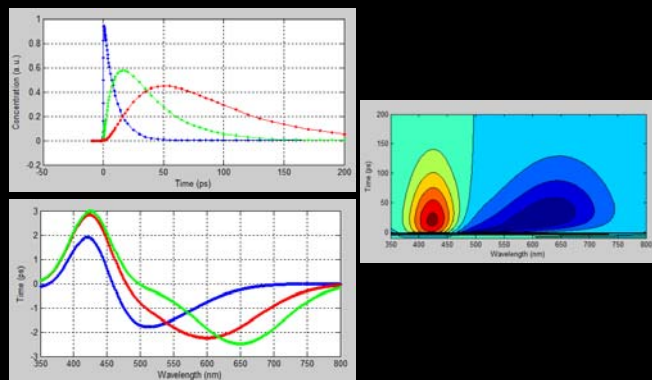
Models describing data for parametrization purposes (global analysis): parallel

State 1 State 2 State 3

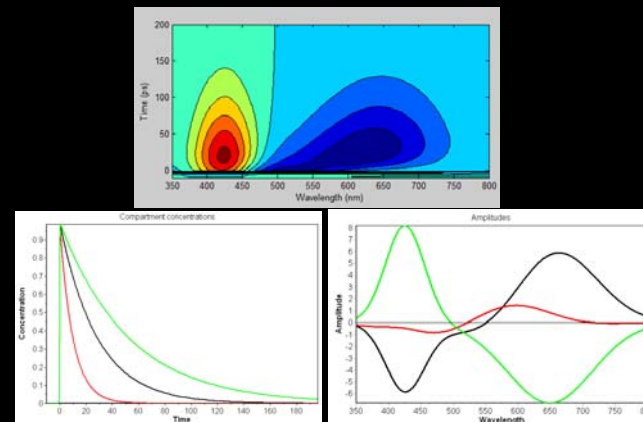


- Independent (parallel) decay model;
- Assumes independent lifetimes for different components;
- Produces *Decay-Associated Difference Spectra*, DADS (in TA) or *Decay-Associated Spectra*, DAS (in fluorescence).
- Negative amplitude means loss of (positive) signal, positive amplitude means gain (growth) of (positive) signal.
- What about the signals with varying signs?

Dataset with varying signs (pump-probe)

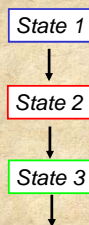


Dataset with varying signs

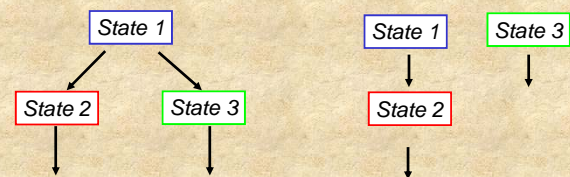


Models describing data for parametrization purposes (global analysis): sequential

- Assumes initial population put in compartment 1, and spectra evolving one into the next.
- Produces *Evolution-Associated Difference Spectra* (EADS).
- Different EADS resemble spectra observed at different times.
- Should be the first model of choice when doing preliminary analysis of TA (and probably fluorescence).



When you start to wonder...



When the different compartments are ascribed physical meanings and connectivity scheme is established using physical assumptions, you are entering the realm of *Target Analysis*.

The resulting spectra with physical meaning are called *Species-Associated Difference Spectra* (SADS)

Build your intuition about SADS:

- Fluorescence SADS should be positive.
- Upon solvation, stimulated emission shifts to the red.
- Ground state SADS are negative only in the GSB region.
- Spectral changes ascribed to different physical processes match your intuition.



Important to remember:

- Not all kinetics are exponential, but most of what we measure can be depicted as such.
- Worse fit and reasonable spectra is better than good fit with ridiculous spectra

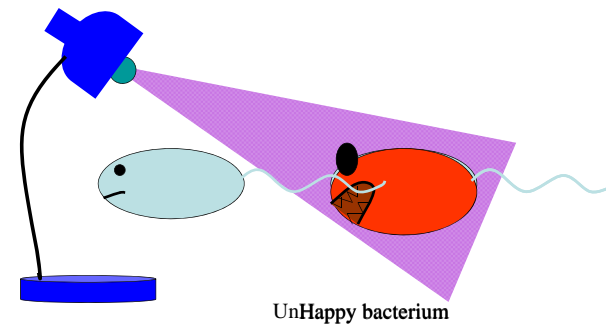


The Photoactive Yellow Protein Structure

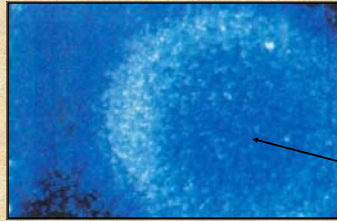
- Function: phototaxis photoreceptor in *Halorhodospira halophila*
- Water-soluble protein, suitable for genetic and chemical engineering
- High-resolution structures available ($\sim 0.85\text{\AA}$)



Negative phototactic response to blue light



*Negative Phototactic Response in
Halorhodospira halophila :
PYP as the signal Transducer*



Negative Phototactic
Response to Applied
Blue Light

Local Light Illumination

Hellingwerf and co-workers: *J Bacteriol*, 1993, 175(10): p. 3096-104.

**Case study:
solvation+isomerization (live demo)**

